

– 1 –

LIMITS FROM *CGRO*/EGRET DATA ON THE USE OF ANTIMATTER AS A POWER SOURCE BY
EXTRATERRESTRIAL CIVILIZATIONS

Michael J. Harris

Universities Space Research Association

300 D Street S.W., Suite 801

Washington DC 20024

U.S.A.

Keywords: Gamma-ray astronomy, antiproton, SETI

I argue that the existence of cold antimatter in bulk is not permitted by the Standard Model, so that if a γ -ray signature from antiproton annihilation were to be detected, it must represent either new physics or the action of intelligence. Time variability of the signal would strongly support the second alternative. The entire sky was scanned at the relevant energies (30 – 928 MeV) by the EGRET experiment on board the *Compton Gamma Ray Observatory* during 1991–1995. A search of this database for the antiproton annihilation signature yielded only upper limits on the flux (an intriguing spectrum detected from QSO 2206+650 = 3EG J2206+6602 is probably not related to SETI). The all-sky, longterm 99% upper limit is 2.3×10^{-8} photon/(cm² s); it is a factor 10 worse in the Galactic plane due to the higher diffuse γ -ray background emission. I give brief, but quantitative, illustrations of what this limit means for nearby intelligent activities.

1. Introduction

It is a quite general consequence of extensions of the Standard Model of particle physics, such as supersymmetry, that the early Universe was characterised by a small excess of baryons over antibaryons [1]. At some point in the cooling of the Big Bang their mutual annihilation produced the enormous photon flux ($\sim 10^9$ photons for each of the few surviving baryons) which we see today as the cosmic microwave background. But regardless of how the baryon excess originated, ordinary Standard Model physics requires that the annihilation process was extremely efficient [2]. It is thus widely believed that no significant numbers of antiprotons (\bar{p}), having survived from the Big Bang, can subsequently have cooled to form substantial "domains" of antimatter, recombining with the corresponding antielectrons (i.e. positrons, e^+).

Any \bar{p} present in the Galaxy today must therefore have been created by well-understood high-energy processes. The energies involved are very large, given the \bar{p} rest-mass ~ 1 GeV, and only one astrophysical environment is adequate – the high energy Galactic cosmic ray flux. The basic physical mechanism involved is for a cosmic ray particle with energy $\gg 2m_pc^2$ incident on a proton at rest in the interstellar medium (ISM) to create a shower of energetic hadrons which may include \bar{p} and pions (neutral π^0 , charged π^+ , π^-) among others.

The $p\bar{p}$ annihilation sites are most germane, since I propose to detect gamma rays from the annihilation process. This may be represented as [3]:

$$p + \bar{p} \rightarrow 2\pi^0 + 1.5\pi^+ + 1.5\pi^- + 0.05K \quad (1)$$

where the multiplicities are average values and K includes all kaon species. The π^0 decay very rapidly into two γ -rays, whose energies in the rest frame are distributed as shown in Fig. 1 [4].

From the considerations above one may conceive of three \bar{p} production processes and their annihilation characteristics:

(1) New physics.

Khlopov et al. [5] among others have proposed an inflationary model with nonhomogeneous baryosynthesis which produces cold antimatter today in regions of sizes of the order of globular clusters (~ 10 pc and $\sim 10^6 M_\odot$). A detailed model of the flux, spectrum and Galactic distribution expected from annihilation of antimatter ejected from these stars has been developed by Golubkov and Khlopov [6], who show that the Galactic halo contains a substantial steady-state population of \bar{p} fed by massive stellar winds and supernova

ejecta. My interest here is in their computed spectrum, which they show to be compatible with EGRET measurements of the γ -ray flux from the halo. The annihilation spectrum of Fig. 1 will be distorted by the velocities of the stars and ejecta (and of \bar{p} accelerated by shocks in the ejecta) and is shown to be much more sharply peaked than Fig. 1. Its distribution is naturally diffuse and steady.

(2) "Hot" cosmic ray antiprotons.

These \bar{p} annihilate in flight with ISM protons, producing a relativistic π^0 and then Doppler-shifted γ -rays. The spectrum of Fig. 1 is kinematically broadened and flattened [7]. It must contribute to the steady diffuse γ -ray background from the Galactic plane at some level, but π^0 can be produced by other high energy reactions, and the amount coming from \bar{p} annihilation will be swamped by decay of π^0 produced directly by the much more common $p + p$ interaction. Even so, the ISM π^0 -decay feature is quite weak, and it is necessarily accompanied by a high level of continuum (smooth spectral power laws) from other high energy proton and electron processes, which tends to swamp it (§2.2).

(3) An artificial source.

The high-energy interactions creating \bar{p} are performed by humans in particle accelerators. It has long been realized that, if practised on a large enough scale, $p\bar{p}$ annihilation could be a very valuable power source for applications requiring portability (e.g. rocket propulsion [8]), that the emission of γ -rays is a signature, and that these γ -rays could be detected [9]. The spectrum would be the cold spectrum of Fig. 1, but its other characteristics are rather speculative; I will assume here that portability implies small size, and so by the usual astronomical argument possible variability. For high-energy gamma ray telescopes, with their bad resolution, small size effectively means a point source. The time-scales on which I searched for variability were ~ 14 d (§2.1).

I conclude that the artificial use of antimatter as a power source has unique characteristics which can be used to identify it, i.e. a "cold" spectrum of the form of Fig. 1 without a sharp peak but narrower than the broad Galactic plane π^0 feature, predominance over any accompanying continuum, and possibly variability. The spectroscopic aspects of this will be discussed further in §2.

The production and cooling of antiprotons by the accelerator technique is inefficient and extremely costly in energy. A back-of-the-envelope calculation shows that gamma rays will only be detectable from an undertaking which is truly immense by human standards (§4.1). However, it is not possible a priori to constrain the nature of the extraterrestrial beings in any way whatever. I do not believe that the scale of the phenomenon can be used as an argument against its possibility. For example, note that processes (1)

and (3) above are not incompatible, in that antimatter might be "mined" on a large scale from a domain by intelligent beings. In this case one might expect to observe both variable and steady annihilation signatures.

Earlier discussions of this topic focused on the role of antimatter in propulsion of extraterrestrial spacecraft [9,10,11]; Harris [12] also made a search for e^-e^+ annihilation powered spacecraft in γ -ray burst data. In this application of antimatter, large Doppler shifts would obviously be another distinctive sign of artificiality. The data to be used here probably do not have sufficient energy resolution for this approach to be used, however (§2.1).

This paper will focus on possibility (3), an artificial source. The evidence for the possibility (1) of new Big Bang physics creating large antimatter domains is thoroughly explored in Ref. [6] and will not be addressed here.

2. Observations and Analysis

2.1. Observations

This paper is based on measurements made by the Energetic Gamma Ray Telescope (EGRET) on board the *Compton Gamma Ray Observatory* (*CGRO*). After launch into low Earth orbit (LEO) in Spring 1991, the mission was divided into Phases of approximately 1 year in length, except for Phase 1 which lasted 18 months. The satellite re-entered on 4 June 2000 during Phase 9. EGRET was fixed at the rear of the spacecraft, and could therefore only be pointed by manoeuvering the whole spacecraft. This was done at approximately 2-week intervals, each pointing being referred to as a Viewing Period (VP).

The physical principles behind the operation of EGRET [13] are shown in Fig. 2 in very schematic form. The key interaction is the formation of a particle-antiparticle pair by an incoming γ -ray photon which has energy $> 2mc^2$. By far the easiest particles to produce are e^- and e^+ , and mc^2 is thus the electron rest mass 0.511 MeV. In practice the cross section for this does not become appreciable until energies of tens of MeV. The cross section is greatly enhanced in the presence of electric charge, which essentially means an atomic nucleus.

The front end of the telescope therefore consisted of a stack of 27 tantalum plates, whose high nuclear charge of 73 enhanced pair creation. In order to actually register a detection ("count"), they were

interleaved with digital spark chambers, i.e. gas-filled chambers with a high voltage across them which suddenly discharge when an e^- or e^+ ionizes a gas molecule. It can be seen from Fig. 2 that the sequence of discharges enables the direction of the photon to be measured. The back end consisted of an array of massive NaI scintillator crystals (the Total Absorption Shower Counter, or TASC) which were intended to stop the e^- and e^+ , so that the total scintillator light (as measured by adjacent photomultiplier tubes) measured the total energy of the photon.

The LEO environment is heavily irradiated by other sources of charged particles, such as Galactic cosmic rays, which can seriously compromise γ -ray measurements, since at these energies they outnumber them by over 1000 to one. Two features of the instrument were designed to mitigate this. First, it was surrounded by an anticoincidence shield, i.e. a large plastic scintillator which, when it detects a particle from the outside, causes the main instrument to be shut off for a very short time (~ 100 ns). Second, fast time-of-flight electronics between the spark chamber assembly and TASC checked the e^- and e^+ trajectories for consistency with an incoming photon before allowing the spark chambers to switch on. The rejection of charged particle backgrounds proved to be extremely efficient, and they never became a problem for EGRET.

Photons in the energy range ~ 30 MeV to 30 GeV can be detected by these processes. Photons with too high energies penetrate the Ta converters without interacting. On the other hand, below 100 MeV the photons tended to be deflected (or even absorbed) by the front end components. This introduced errors into EGRET low-energy measurements which could never be fully corrected for, and which had an impact upon my analysis (§3).

The energy resolution of EGRET was poor. The photons were binned into ten energy channels which are listed in Table 1. Only channels 0-8 were used in my analysis. The poor resolution ($> 50\%$ above 100 MeV) made measurements of Doppler shifts unrealistic.

The accuracy of photon direction measurement (equivalent to point spread function [PSF]) varied strongly with photon energy, from several degrees below 100 MeV to 0.8° at 1 GeV; for the energies of Fig. 1 the average value was about 2.5° . It also varied with distance from the centre of the field of view (FOV), which was $\sim 80^\circ$; sensitivity and PSF were poor at off-axis distances $> 30^\circ$. Angular resolutions actually achieved in analysis are of course much better if there are enough counts.

A major constraint on the capabilities of EGRET was the availability of the Ne/Ar gas mix used in the spark chambers; being non-renewable, this began to run out at the end of Phase 4 (October 1995), after

which EGRET was used as little as possible. I have used data from Phases 1–4 in my analysis.

The EGRET instrument team have presented their data in the form of maps for each VP, and for the combined Phase 1–4 data, for three quantities: the raw count numbers, the γ -ray intensities (i.e. count rate per unit live time, per unit area, per unit energy, using an effective area weighted for the detection efficiency, PSF and location in the FOV), and the exposure (essentially, the variation of the live time across the map). The maps are on a $0.5^\circ \times 0.5^\circ$ grid. They are readily available in zipped form via FTP; see <http://cossc.gsfc.nasa.gov/cossc/EGRET>. I searched the Phase 1–4 sum spectra from the entire sky for an annihilation signature.

2.2. Analysis Principles

When binned into the EGRET energy channels of Table 1, the $p\bar{p}$ annihilation spectrum of Fig. 1 appears as in Fig. 3. This strongly suggests that a search for that spectrum should begin by selecting map locations with excess counts in EGRET channel 4. Before applying this criterion naively, it is necessary to consider possible backgrounds which might affect these energies (150–300 MeV).

Instrumental backgrounds are low (§2.1). The relevant background here is the entirety of known cosmic γ -ray sources. In general this means known and measured large-scale diffuse fluxes from the Universe at large and from the Galactic halo, plane and solar vicinity. The measurement of these was a major objective of the EGRET experiment, but for my analysis they were a nuisance. The salient features of these spectra are the following.

The extragalactic background and halo-plus-local (defined as $|b| > 10^\circ$) spectra were separated from each other by [14], who measured the sum of them as a function of latitude b , and extrapolated to 90° (this is more accurate than any single measurement of the extragalactic emission at 90°). In this way, the extragalactic background spectrum was found to be a power law of index -2.1. A power-law index ~ -2 is observed from the halo due to cosmic ray proton and electron processes in the ISM [15]. Only the combined halo-plus-extragalactic spectrum was needed for my analysis, which I assumed to be a power law of index ~ -2 .

The strength of this spectrum increases as b decreases. This is true in a much more marked way of the emission associated with the Galactic plane (the component with $|b| < 10^\circ$). Since by far the bulk of

the ISM resides in the plane, this component is very intense, which made it much easier for EGRET to measure details of its spectrum. Thus, superimposed on the power law of index ~ -2 which comes from typical cosmic ray-ISM interactions EGRET detected two features: a broad but weak peak centred at a few hundred MeV, merging into a general excess of emission at energies above 1 GeV. The former might be the spectrum from relativistic π^0 decay (§1); the latter is unexplained [16,17].

Of these various spectral features, which are important at various latitudes, only the power laws were a significant background problem for my analysis. In principle the broad π^0 decay feature from the ISM in the Galactic plane might contaminate any extraterrestrial candidate $p\bar{p}$ spectrum from a point source; however in practice it is too weak on spatial scales $\sim 1^\circ$ relative to the strong continuum, and the shape is too dissimilar (it is much broader). I did not consider energies significantly above 1 GeV and therefore neglected the alleged excess. I thus had to take into consideration contamination from a power-law spectrum whose intensity rose sharply in and near the Galactic plane.

Some effects of this can be seen in Fig. 4, which shows schematically a power law superimposed on the $p\bar{p}$ annihilation spectrum. First, it is clear that the annihilation spectrum is completely dominated by the power law at energies below 100 MeV (EGRET channels 0–2); therefore channels 3, 4 and 5 only will play a role in detection. Second, although Fig. 3 shows that channel 4 in general contains the most counts, the *contrast* between the annihilation function and the power law is greatest in channel 5. Third, the power law itself is not very well characterised; it is "anchored" at the high-energy end by channels 6–8, none of which in general contains many counts, and at the low-energy end by channels 0–2, which are subject to systematic errors (§2.1).

2.3. Analysis (Details)

The considerations in §2.2 were taken into account in the design of the analysis. My overall strategy was to search the EGRET Phase 1–4 sky map point by point for spectra of the form of Fig. 4. This tacitly assumes that the source(s) have a large duty cycle (§4). When a source was detected, I went back to the individual EGRET VPs which covered the same region of the sky. A measurement of the same form of spectrum was made in each VP and the results were arranged in a time series. A variable level would strengthen the case for an candidate extraterrestrial power source (§1).

The process involved several steps:

(1a) The EGRET PSF was crudely approximated by a uniform circle of radius 2.5° centred on each grid point in the EGRET Phase 1–4 map. The spectral intensities from each point within the circle were averaged over. The counts from each point were summed. Attention then turned to the next point in the grid 0.5° away, in the manner of Fig. 5. This procedure assumes that the measurement precision is limited by small-number statistics.

(1b) This procedure was modified within 8.5° of the Galactic plane, where many counts were registered even within single 0.5° grid points. If several sources occur within the PSF circle then measurement is confusion-limited by this contamination, and it is better to measure the spectra from the individual grid points.

(1c) In both cases an error equal to the square root of the counts was assigned to each channel. Typically the cut at $|b| = 8.5^\circ$ corresponded to a level of several tens of counts in channel 4.

(2) An automated search selected those spectra which had a peak at channel 4 in counts. Channels 2 and 3 were constrained to be less than channel 4, channel 5 was constrained to be less by a factor 2 (Fig. 3).

(3) Many of these spectra turned out to be unusable for various reasons, for example zero counts in one or more channels. The selected spectra were examined visually for these problems. The criterion used was that an excess in channel 5 be visible, since this channel contrasts best against a power law background.

(4) It is obvious from Fig. 5 that most of the spectra generated in step 1a are not independent measurements, since successive PSF circles overlap. Away from the Galactic plane ($|b| > 8.5^\circ$) clusters of the selected spectra in $\sim 2.5^\circ$ groupings were identified, from each of which a single representative spectrum at or near the centre was retained. A large majority of the selected spectra fell into these groupings, which suggests that the selection process was not discovering statistical fluctuations in counts.

(5) The surviving candidate spectra were fitted with a spectral model consisting of the annihilation function plus a power law (as in Fig. 4). The fits were performed by the IDL utility nonlinear least-squares fitting routine CURVEFIT.

(6) If a candidate point showed a significant level of $p\bar{p}$ annihilation emission, the individual VPs contributing to the Phase 1–4 spectrum were examined for variability or constancy. The positions of known EGRET sources were excluded as being background, and presumably having been examined already [18].

Table 2 shows the number of candidates resulting from each of these steps.

3. Results

The amplitudes returned by CURVEFIT for the $p\bar{p}$ annihilation function represent the results. The average results for the two zones $|b| > 8.5^\circ$ and $|b| < 8.5^\circ$ are shown in Table 2. Before going into more detail, a comment on the errors is necessary.

The errors are clearly much larger in the Galactic plane. This is readily understood in terms of the background level (§2.2). In terms of Fig. 4, the underlying power law is elevated by more than an order of magnitude, and the annihilation function becomes invisible against it. Out of the plane there is a weaker rising background as the plane is approached, but another source of error — poor statistics due to lesser EGRET exposure — dominates in the high-latitude regions where this background is low. These two effects work in opposite directions in b , so that above $|b| = 8.5^\circ$ the error is not a strong function of latitude. Quoting an average value for the error as in Table 2 is therefore meaningful.

The criterion as to whether an annihilation signature has been detected at any point is the significance σ of the measurement over and above the estimated error (of which average values at 99% confidence are quoted in Table 2). Rather than absolute intensities, I therefore plot in Fig. 6 the distribution of the results in standard deviations. If the measurement errors were randomly distributed, this would in general be a Gaussian of mean 0 and standard deviation 1; it is obvious, however, that the strong selection procedures which I applied in §2.3 in order to isolate a positive result have heavily biased the distribution towards positive values. Hence the measured distribution of significances is the high- σ "tail" of a hypothetical distribution of all measurements (including points that were rejected by my selection procedure and never measured). If the errors were randomly distributed about a null result this hypothetical distribution would be a Gaussian distribution of mean zero and standard deviation 1 normalized to the number of possible independent EGRET PSFs. Given the Cartesian 0.5° EGRET gridding and my approximation of the PSF by a 2.5° circle there are $\sim 720 \times 360 / (\pi \times 5^2) = 3300$ independent PSFs.

The high- σ "tail" of this expected distribution is overplotted in Fig. 6. It is clear that there are a significant number of measured values in excess of what is expected ($\sigma > 2.5$; see also Table 2, step 5). I compared the corresponding spectra with typical ones within the expected range of significances; examples of the two types are shown in Figs. 7a and 7b. In almost all cases, the supposedly high- σ annihilation features were clearly artefacts of anomalous count rates in EGRET channels 0–2. For example, it is clear in Fig. 7b that, if there were not an anomalous low flux in channel 0, the spectrum would be well fitted by a power law. Since, as pointed out in §2.1, channels 0–2 are subject to poorly-understood systematic errors, I

conclude that the measurements of highly significant $p\bar{p}$ annihilation fluxes in Fig. 6 are in general spurious.

The only spectrum remaining after I had rejected those with problems in channels 0–2 was peculiar. At location $l = 107.25^\circ$, $b = 11.5^\circ$, a Phase 1–4 spectrum was obtained which did not show obvious systematics in channels 0–2 and which showed the annihilation feature at a significance 3.8σ (a nominal probability of $\sim 2 \times 10^{-4}$ of occurring by chance); however, there was an unexpected excess in channel 7 (Fig. 7c). This is in fact the quasar QSO 2206+650, which was detected by EGRET (3EG J2206+6602, [19]), and the source should probably be rejected as an ETI candidate for both of these reasons. As an illustration of the procedure which might in future be applied as an ETI test using variability (§2.3, analysis step 6), I fitted the usual power-law plus $p\bar{p}$ model to the EGRET spectra from the 9 VPs in which $l = 107.25^\circ$, $b = 11.5^\circ$ was within the FOV. Interestingly the $p\bar{p}$ light curve apparently shows variability (Fig. 7d), which would have been a characteristic of ETI activity.

4. Discussion

4.1. Annihilation Flux Limits

The search performed here is essentially complete and homogeneous in space. I therefore adopt an upper limit on the steady $p\bar{p}$ annihilation flux of 2.3×10^{-8} photon/(cm² s) from any point outside the Galactic plane, with a limit about a factor 10 higher in the plane. The upper limit on transient fluxes is less easily established. My search method was designed for steady sources or those with a high duty cycle — i.e., a duty cycle long enough that the transient emission dominates the overall Phase 1–4 emission. Since a short, strong event of low duty cycle (1 VP) will do this, as will a long, slow, weak event lasting for years, one must choose a "standard" duty cycle, and determine the corresponding "standard" flux limit.

Let us consider the behaviour of the source at $l = 107.25^\circ$, $b = 11.5^\circ$ (Fig. 7d) as a test case. This source is known to produce a detectable annihilation flux when averaged over Phases 1–4 (Fig. 7c). My fitting of the power-law plus annihilation spectrum to each VP where this point was visible to EGRET showed that the spectral anomaly apparently occurred in more than one event of amplitude $\sim 10^{-7}$ photon/(cm² s) on a characteristic timescale ~ 100 d. This is a good example of how variability was clearly detected with a particular duty cycle, so I adopt its parameters as standard, for convenience. They are close to the approximation that the error varies inversely with the square root of the elapsed time, which

is true for Gaussian counting errors. I conclude that the general upper limit on transient $p\bar{p}$ annihilation fluxes is $\sim 10^{-7}$ photon/(cm² s) for duty cycles $\sim 1/16$ of Phases 1–4 (i.e. 100 d), is scaled by a factor ~ 10 in the Galactic plane, and in general varies roughly as the reciprocal of the square root of the time-scale of transient.

In terms of ETI activity at an unknown distance R pc, the above numbers translate into the consumption of $\sim 1\text{--}5 R^2$ ton/s of antiprotons, or $\sim 10^8 R^2$ tons total. The value of R is completely undetermined; as an example, ETI activity within the Oort cloud at ~ 0.25 pc would be detectable if it involved $\sim 5 \times 10^6$ ton of antiprotons on the time-scales discussed above. This is about 15 orders of magnitude in excess of what could be expected to be produced on Earth in the near future [20].

My result may be compared with the predictions of earlier authors, taking into account the different combinations of antimatter mass and distance R which they used. Thus Matloff and Mallove [21] considered a rocket with payload mass 10^{10} kg, $\Delta v = 0.2c$ and acceleration time 10 yr, which would burn \bar{p} at a rate of 1 kg/s. At their reference distance of 10 pc it would be quite undetectable; EGRET would have detected it at 10^{12} km = 6500 AU. A more modest proposal for a crewed mission to α Centauri (5000 ton payload on first leg of a 20-year return mission, accelerating at 1 g to 0.245 c in 3 months, [22]) burns a smaller amount of p- ($\simeq 15000$ tons) on a shorter time-scale and is detectable at a similar distance, 4500 AU.

My result may also be compared with the detectability radii for present-day human-planned interstellar spacecraft, i.e. the fusion-powered Daedalus [23] and Orion [24] designs; by a variety of X-ray, gamma-ray, EUV and neutron detection techniques, these craft were found to be detectable at ranges up to only 10^9 km [10]. Presumably the antimatter propulsion mission to α Cen suggested by Forward (1 ton payload one-way, 180 kg \bar{p} consumed in < 1 yr [11]), being much smaller, would be more difficult to detect by these conventional means. However EGRET would have detected it at a similar distance, 1.5×10^9 km = 10 AU. In human terms, the missions proposed in [10] and [22] can perhaps be thought of as the most primitive possible uncrewed and crewed antimatter missions, respectively, to α Cen.

4.2. Towards an Improved Measurement

There are several approaches which might be explored in order to improve upon this result. An immediately practicable one would be to search for low duty cycle transients in the EGRET data. As emphasised in §4.1 my search in the average Phase 1–4 data had some sensitivity to constant sources and

those of duty cycle $\geq 1/16$. A search in the individual VP data might discover transients on much shorter time-scales. This would involve performing the analysis steps 1–6 of §2.3 on all of the 170 individual VPs in Phases 1–4.

Improvements in future high energy γ -ray telescopes would obviously lead to better results. The problems reported in §3 with EGRET channels 0–2 show that sensitive and calibrated responses are a critical requirement at energies 30–100 MeV in order to determine the power-law background. Better energy resolution overall would enable the shape of the feature, which I defined in terms of channels 4 and 5 and assumed to be due to $p\bar{p}$ annihilation, to be determined more accurately. A larger effective area would obviously increase the sensitivity of the search. These improvements will be achieved by the upcoming Gamma-Ray Large Area Space Telescope (GLAST [25], planned for 2006), with 15 times the sensitivity of EGRET and ~ 5 times its energy resolution.

5. Conclusion

I conclude that it is practicable to measure $p\bar{p}$ annihilation spectra separately from underlying power-law backgrounds if the appropriate selection criteria are applied. By hypothesis, any source emitting this spectral feature must be artificial; it is extremely difficult to imagine any other possibility except new laws of physics (§1). When applied to the EGRET data the method would have detected a steady $p\bar{p}$ annihilation spectrum down to levels $\sim 2 \times 10^{-8}$ photon/(cm² s), and transients on time-scales ranging down to ~ 100 d at levels ranging up to $\sim 10^{-7}$ photon/(cm² s), outside the Galactic plane, both numbers being about a factor 10 higher in the plane. Variable emission detected from the known extragalactic source QSO 2206+650 is presumably not related to ETI activity.

These results, limited though they are, are the first ever obtained in this field. They exclude the presence of "human-scale" antimatter-powered space probes (such as might be constructed by humans in this century [11]) within a radius of ~ 10 AU, and more ambitious human-like crewed interstellar craft out to several thousand AU. They will be greatly improved by future high energy γ -ray missions such as GLAST.

I would like to thank the EGRET PI team and Seth Digel in particular for creating an excellent archive. I am grateful to Prof. Sherry Cady of Portland State University for obtaining criticisms of a

previous version of this paper.

References

1. A. Riotto and M. Trodden, "Recent progress in baryogenesis", *Annual Review of Nuclear and Particle Science*, 49, pp.35–75, 1999.
2. Ya. B. Zel'dovich and I. D. Novikov, I. D., *Relativistic Astrophysics, Vol. 2. The Structure and Evolution of the Universe*, ed. G. Steigman, University of Chicago Press, Chicago, pp.163–170, 1983.
3. C. Baltay, P. Franzini, G. Lütjens, J. C. Severiens, D. Tycko, and D. Zanotto, "Annihilation of antiprotons at rest in hydrogen. V. Multipion annihilations", *Phys. Rev.*, 145, pp.1103–1111, 1966.
4. G. Backenstoss et al., "Proton-antiproton annihilations at rest into $\pi^0\omega$, $\pi^0\eta$, $\pi^0\gamma$, $\pi^0\pi^0$, and $\pi^0\eta'$ ", *Nuclear Physics*, B228, pp.424–438, 1986.
5. M. Yu. Khlopov, S. G. Rubin, and A. S. Sakharov, "Possible origin of antimatter regions in the baryon dominated universe", *Phys. Rev.*, D62, 083505, 2000.
6. Yu. A. Golubkov and M. Yu. Khlopov, "Antiprotons annihilation in the Galaxy as a source of diffuse gamma background", *Physics of the Atomic Nucleus*, 64, pp.1821–1829, 2001.
7. R. R. Hillier, *Gamma ray astronomy*, Oxford University Press, Oxford, p.13, 1984.
8. I. A. Crawford, "Interstellar travel: a review for astronomers", *Quarterly Journal of the Royal Astronomical Society*, 31, pp.377–400, 1990.
9. M. J. Harris, "On the detectability of antimatter propulsion spacecraft", *Astrophysics and Space Science*, 123, 297–303, 1986.
10. D. R. J. Viewing, C. J. Horswell, and E. W. Palmer, "Detection of starships", *JBIS*, 30, pp.99–104, 1977.
11. R. L. Forward, "Antimatter propulsion", *JBIS*, 35, pp.391–395, 1982.
12. M. J. Harris, "A search for linear alignments of gamma-ray burst sources", *JBIS*, 43, pp.551–555, 1990.
13. D. J. Thompson et al., "Calibration of the Energetic Gamma-Ray Experiment Telescope (EGRET) for the Compton Gamma-Ray Observatory", *Astrophys. J. Suppl. Ser.*, 86, pp.629–656, 1993.
14. P. Sreekumar et al., "EGRET observations of the extragalactic gamma-ray emission", *Astrophys. J.*, 494, pp.523–534, 1998.
15. S. D. Hunter et al., "EGRET observations of the diffuse gamma-ray emission from the Galactic plane",

Astrophys. J., 481, pp.205–240, 1997.

16. A. W. Strong, I. V. Moskalenko, and O. Reimer, "Diffuse Galactic continuum gamma rays", in *The Fifth Compton Symposium*, ed. M. L. McConnell and J. M. Ryan, American Institute of Physics Proceedings 510, pp.283–290, 2000.
17. S. W. Digel, S. D. Hunter, I. V. Moskalenko, J. F. Ormes, and M. Pohl, "The origin of cosmic rays and the diffuse Galactic gamma-ray emission", in *Gamma 2001*, ed. S. Ritz, N. Gehrels, and C. R. Shrader, American Institute of Physics Proceedings 587, pp.449–458, 2001.
18. D. Petry, "A first EGRET-UNID-related agenda for the next-generation Cherenkov telescopes", in *Proceedings, The Nature of Unidentified High-Energy Gamma-Ray Sources*, ed. A. Carraminana, O. Reimer and D. J. Thompson, Kluwer Academic, Dordrecht, pp.299–319, 2001.
19. R. C. Hartman et al., "The third EGRET catalog of high-energy gamma-ray sources", *Astrophys. J. Suppl. Ser.*, 123, pp.79–202, 1999.
20. G. R. Schmidt, H. P. Gerrish, J. J. Martin, G. A. Smith, and K. J. Meyer, "Antimatter requirements and energy costs for near-term propulsion applications", *Journal of Propulsion and Power*, 16, pp.923–928, 2000.
21. G. L. Matloff and E. F. Mallove, "Alien starship detectability: bursters and skidmarks", 39th Congress of the International Astronautical Federation, October 8–15 1988, Bangalore, Paper IAA-88-552, 1988.
22. B. N. Cassenti, "Design considerations for relativistic antimatter rockets", *JBIS*, 35, pp.396–404, 1982.
23. A. Bond and A. R. Martin (eds), *Project DAEDALUS*, British Interplanetary Society, London, 1978.
24. J. C. Nance, "Nuclear Pulse Propulsion", *IEEE Transactions on Nuclear Science*, NS-10, pp.177–182, 1965.
25. P. F. Michelson, "The Gamma-ray Large Area Space Telescope mission: science opportunities", in *Gamma 2001*, ed S. Ritz, N. Gehrels, and C. R. Shrader, American Institute of Physics Proceedings 587, New York, pp.713–721, 2001.

Channel number	0	1	2	3	4	5	6	7	8	9
Lower edge [1]	30	50	70	100	150	300	500	1000	2000	4000
Upper edge [1]	50	70	100	150	300	500	1000	2000	4000	10000

Note:

1. Energies in units of MeV

Table 1: EGRET energy channels

Zone	Step 1	Step 2	Step 3	Step 4	Step 5	Step 6	Flux, [2]
[1]							photon/(cm ² s)
$ b > 8.5^\circ$	234270	8492	3456	387	12	1	$< 2.3 \times 10^{-8}$
$ b \leq 8.5^\circ$	24480	1639	138	138	29	0	$< 2.6 \times 10^{-7}$

Notes:

1. $|b| \leq 8.5^\circ$ is the Galactic plane.
2. Flux 99% confidence upper limit.

Other table entries represent the number of sources surviving each step in the selection procedure.

Table 2: Search statistics, and results

Fig. 1.— Normalized spectrum of photons resulting from "cold" antiproton annihilation; an analytic formula is given by [4].

Fig. 2.— Simplified diagram of EGRET. Overall dimensions 1.65 m diameter \times 2.25 m height. Dashed line - incoming photon. Full lines - e^- and e^+ generated by pair production within Ta layer. TOF = time of flight.

Fig. 3.— The $p\bar{p}$ annihilation spectrum of Fig. 1 binned into the EGRET energy channels from Table 1.

Fig. 4.— Schematic illustration of the spectrum resulting from a $p\bar{p}$ annihilation signal (Fig. 1) superimposed on a power-law background. Dashed lines - individual components. Full line - sum of the two components. Numbers at top of figure represent the weighted mean energies of the EGRET channels. For ease of illustration, the amplitude of the annihilation spectrum is much greater than a typical case from my selected spectra.

Fig. 5.— Procedure for accumulating EGRET spectra for points away from the Galactic plane (schematic). Intensity at a point A = average intensity measured over all points within the approximated EGRET PSF (full circle, radius 2.5°). Counts at point A = sum of all counts registered within the circle. The procedure is repeated at every grid point (dashed circles centred at B, C...).

Fig. 6.— Histogram - distribution of 525 measured $p\bar{p}$ annihilation amplitudes in terms of their statistical significances (amplitude divided by statistical error). Full line - part of the expected distribution for measurements randomly (normally) distributed around a null result. Note the positive offset of the measured distribution and the excess of measurements above the full line for significances $> 2.5\sigma$.

Fig. 7.— (a) A typical EGRET spectrum, showing weak or no $p\bar{p}$ annihilation feature. Phase 1–4 spectrum, $l = 117.25^\circ$, $b = 11.75^\circ$. Data points - intensities in EGRET channels 0–8. Full line - spectral model fit with power-law plus annihilation function (Figs. 1, 4) of amplitude $0.29 \pm 1.08 \times 10^{-8}$ photon/(cm 2 s). (b) Spectrum showing a spurious annihilation feature (full line) due to a systematic error in channel 0, such as is responsible for most of the measurements with significance $> 2.5\sigma$ in Fig. 6. Phase 1–4 spectrum, $l = 197.25^\circ$, $b = 25.25^\circ$, $p\bar{p}$ amplitude $2.88 \pm 0.45 \times 10^{-8}$ photon/(cm 2 s). Dashed line — power law fit to channels 1–8. (c) Phase 1–4 spectrum of candidate object $l = 107.25^\circ$, $b = 11.5^\circ$, rejected due to identification with QSO 2206+650. Annihilation amplitude $5.05 \pm 1.19 \times 10^{-8}$ photon/(cm 2 s). (d) Variability of flux from $l = 107.25^\circ$, $b = 11.5^\circ$, from measurements during each VP (top label) when the point was within the EGRET aperture. Dashed line — overall amplitude 5.05×10^{-8} photon/(cm 2 s) during Phases 1–4 from (c). Mission day 0 = 16 May 1991.

Figure 1

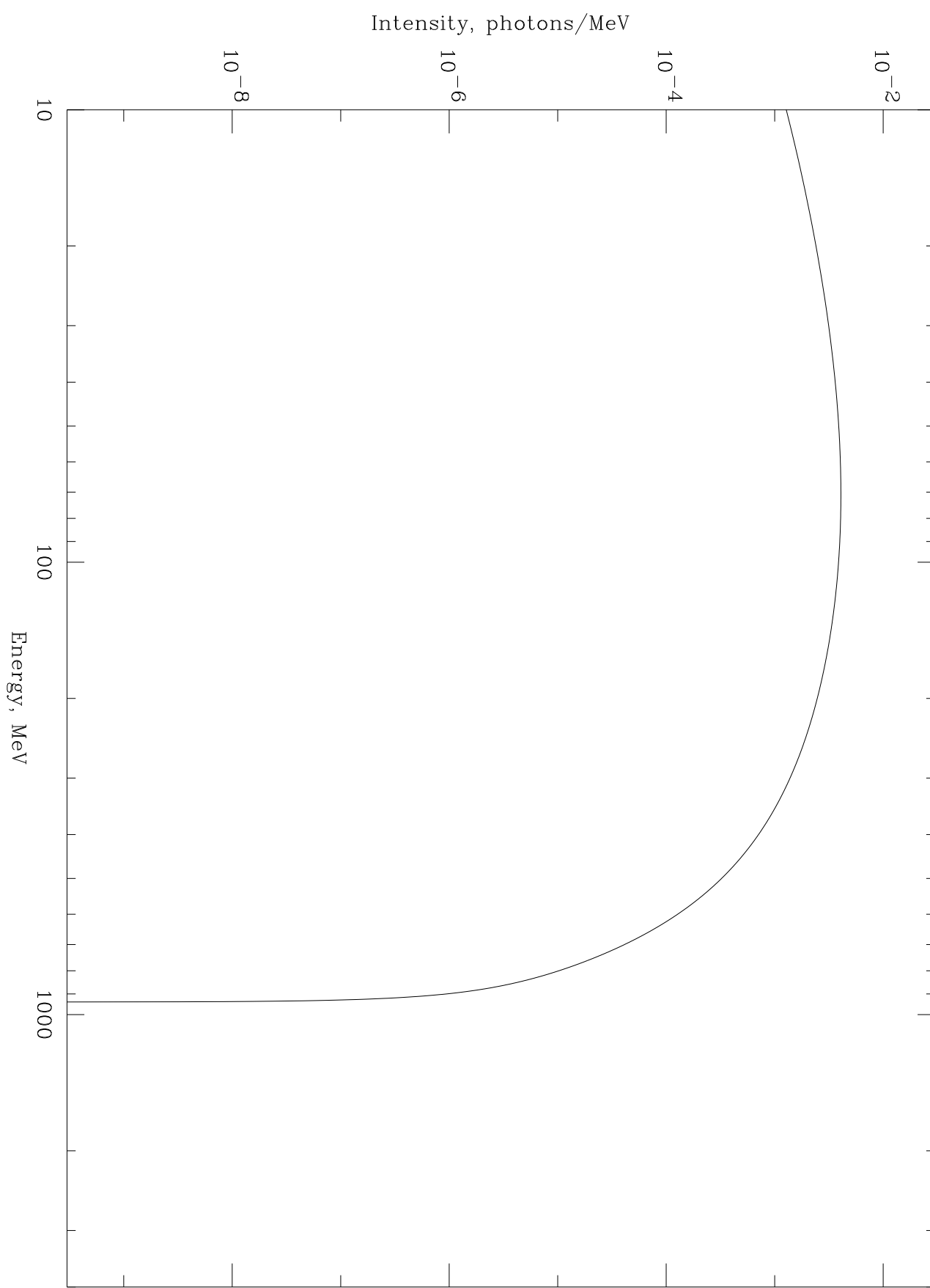


Figure 2

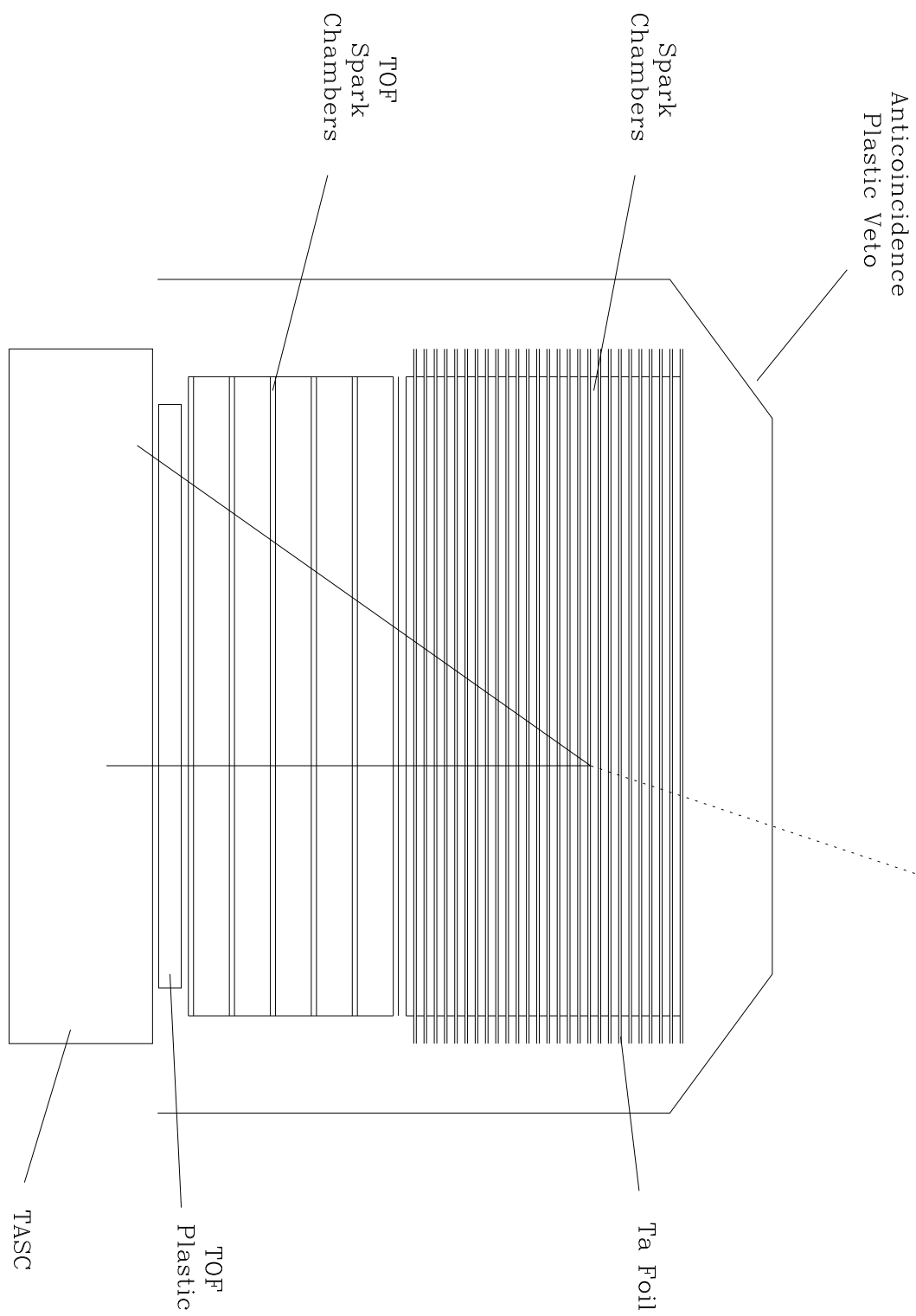


Figure 3

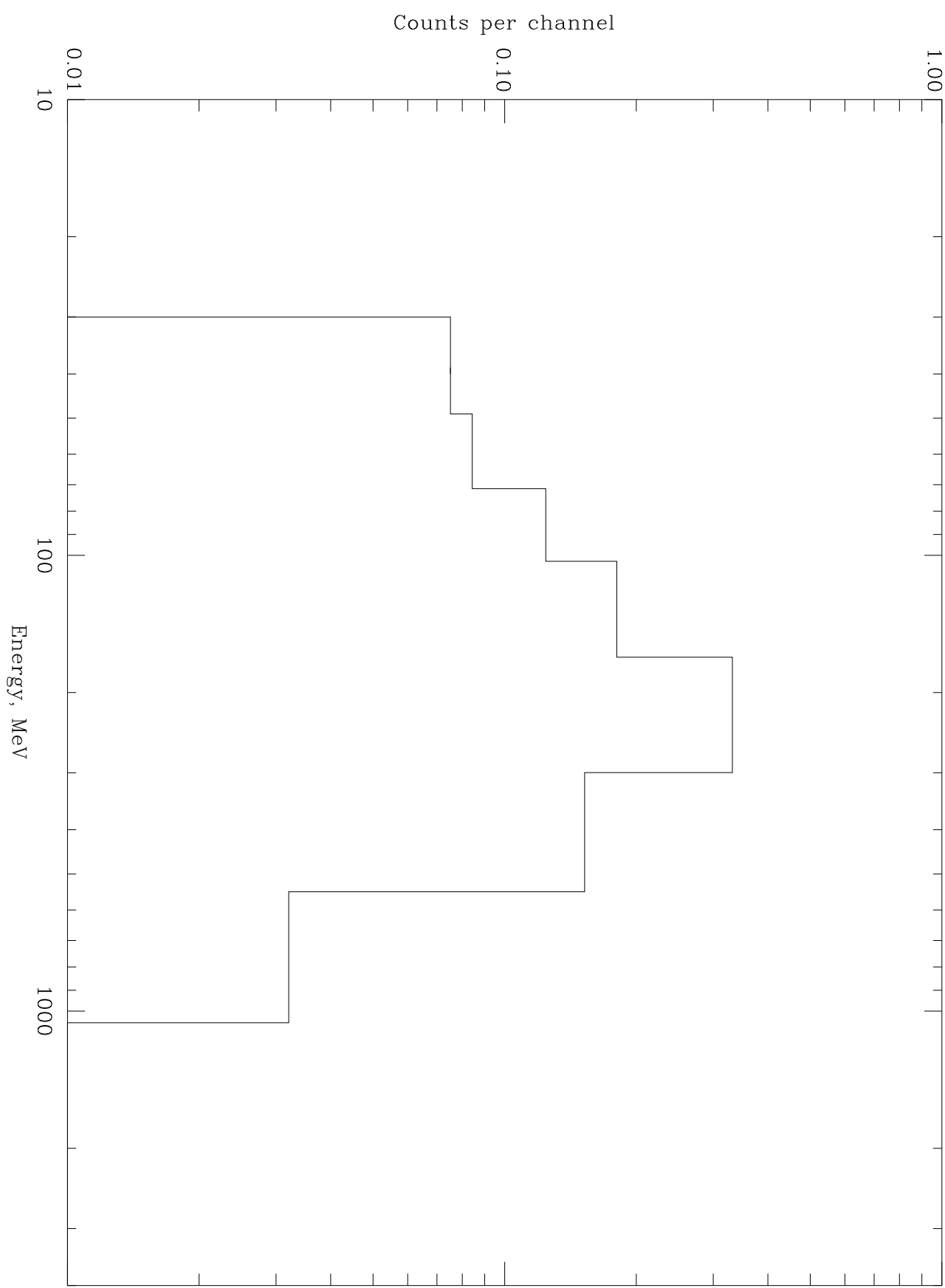


Figure 4

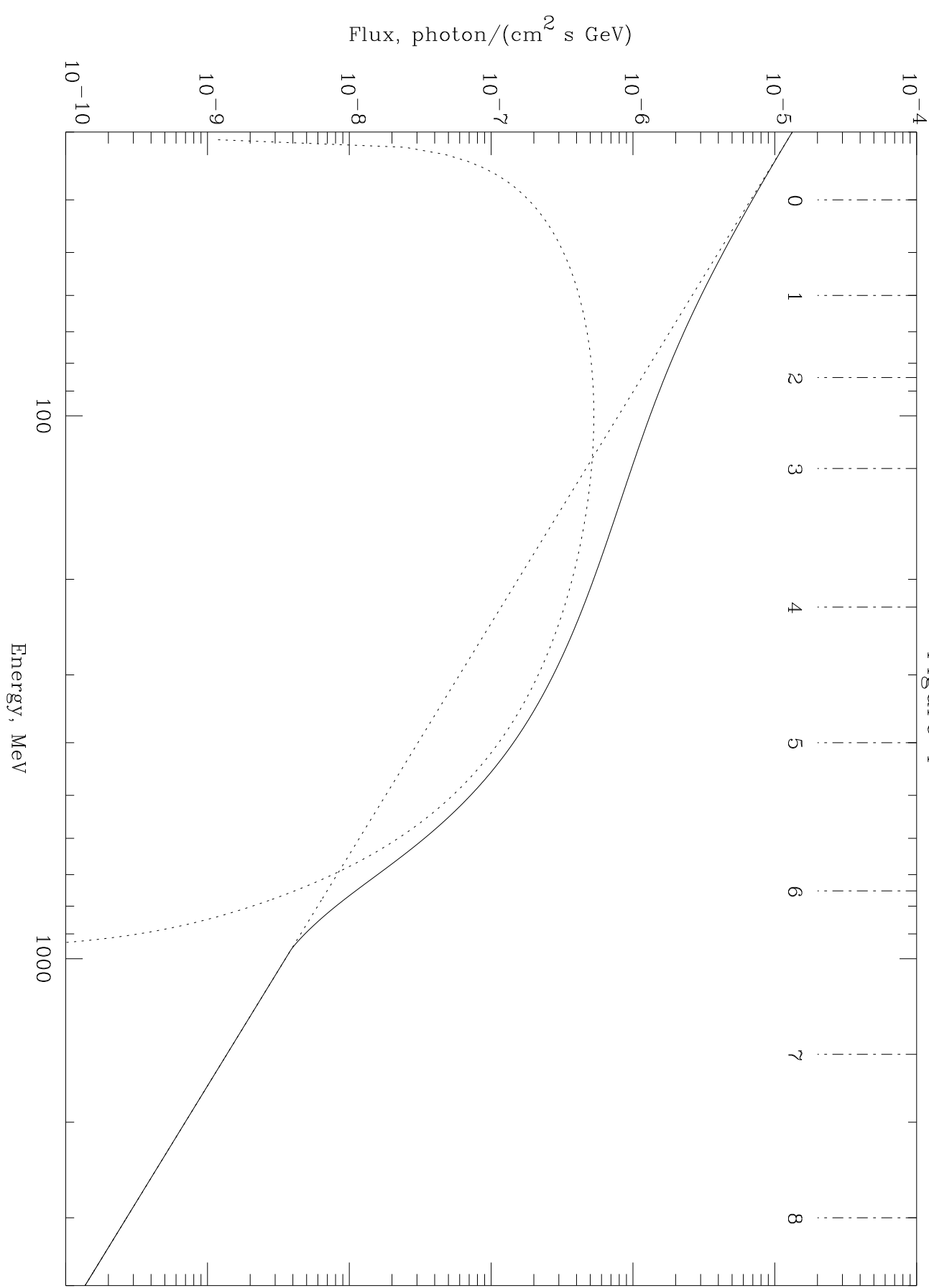


Figure 5

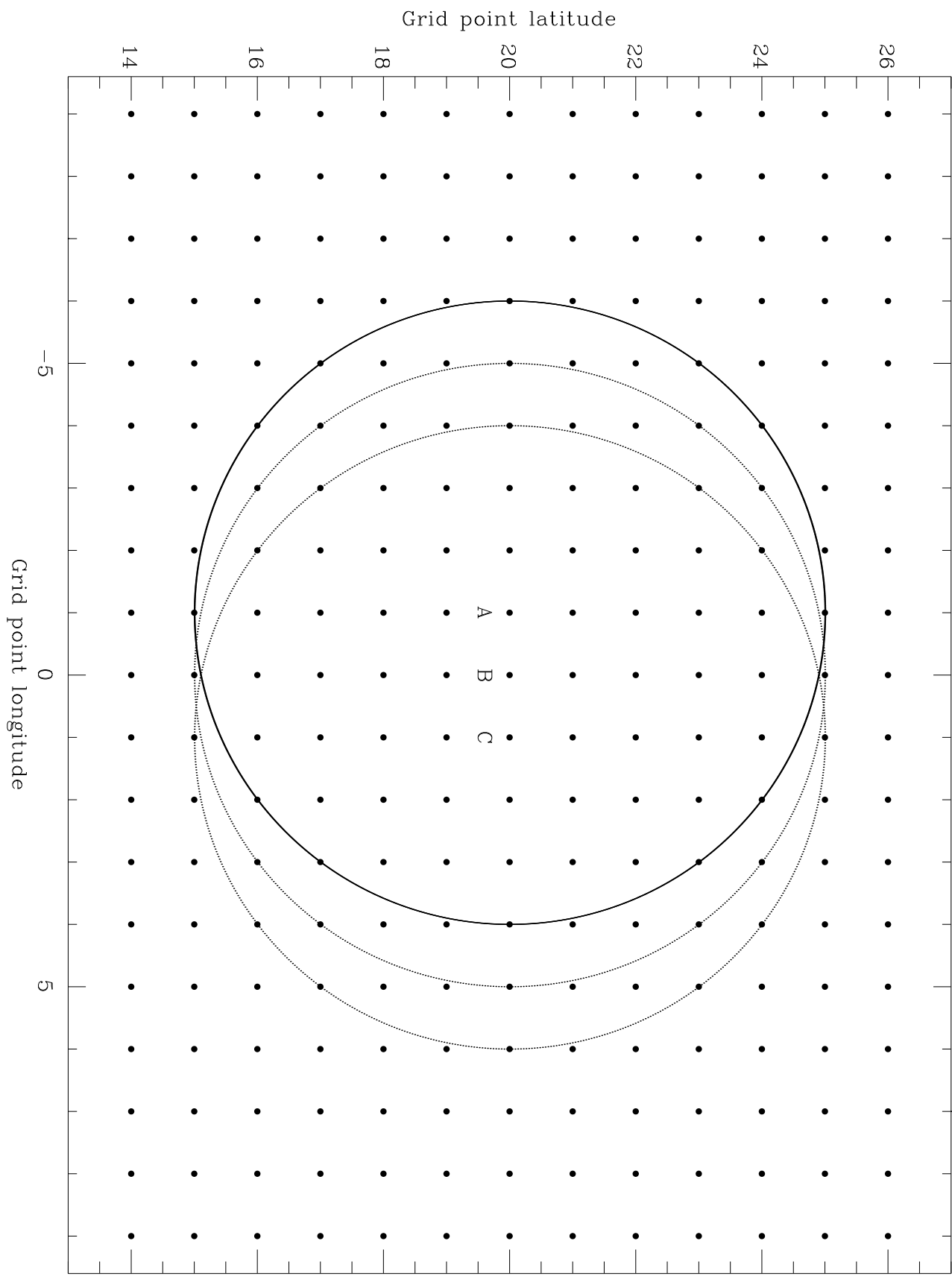


Figure 6

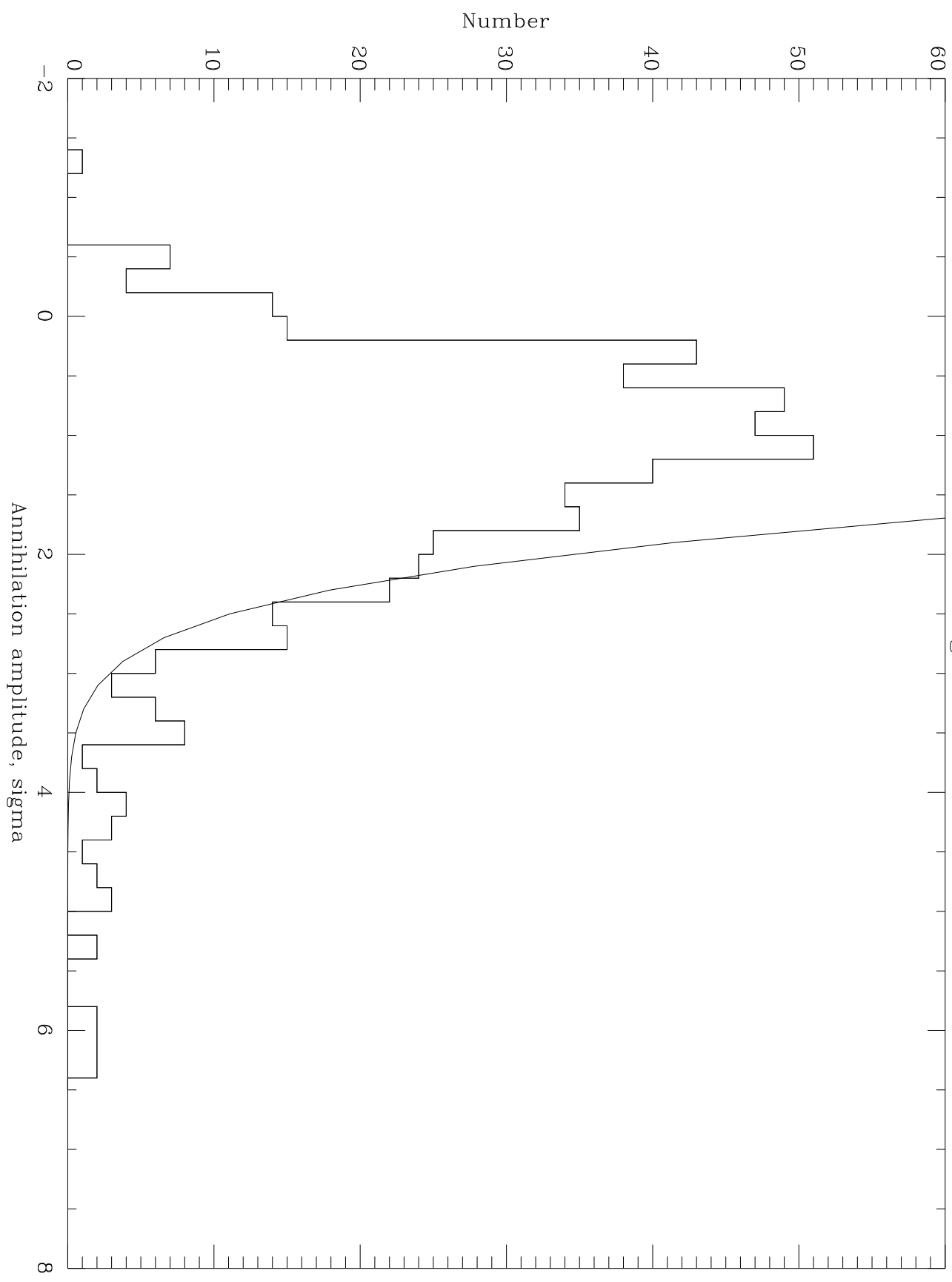


Figure γ

10⁻⁵
10⁻⁴

a

b

Flux, photon/(cm² s GeV)

10⁻⁵
10⁻⁶
10⁻⁷

10⁻⁷
10⁻⁸
10⁻⁹

10⁻⁹

100
1000

Energy, MeV

10⁻⁵
10⁻⁶
10⁻⁷

10⁻⁷
10⁻⁸
10⁻⁹

10⁻⁹
10⁻¹⁰
10⁻¹¹

10⁻¹⁰
10⁻¹¹
10⁻¹²

1.5x10⁻⁷
1.0x10⁻⁷
5.0x10⁻⁸

0
-5.0x10⁻⁸
-1.0x10⁻⁷

VP 2
22
34
203
211
212
302
401

100
1000

Energy, MeV

